

## Electronic structure of $\beta$ -RbNd(MoO<sub>4</sub>)<sub>2</sub> by XPS and XES

V.V. Atuchin <sup>a,b,c,\*</sup>, O.Y. Khyzhun <sup>d</sup>, O.D. Chimitova <sup>e</sup>, M.S. Molokeev <sup>f</sup>, T.A. Gavrilova <sup>g</sup>, B.G. Bazarov <sup>e</sup>, J.G. Bazarova <sup>e</sup>

<sup>a</sup> Laboratory of Optical Materials and Structures, Institute of Semiconductor Physics, SB RAS, Novosibirsk 630090, Russia

<sup>b</sup> Functional Electronics Laboratory, Tomsk State University, Tomsk 634050, Russia

<sup>c</sup> Laboratory of Semiconductor and Dielectric Materials, Novosibirsk State University, Novosibirsk 630090, Russia

<sup>d</sup> Frantsevich Institute for Problems of Materials Science, National Academy of Sciences of Ukraine, Kyiv UA-03142, Ukraine

<sup>e</sup> Laboratory of Oxide Systems, Baikal Institute of Nature Management, SB RAS, Ulan-Ude 670047, Russia

<sup>f</sup> Laboratory of Crystal Physics, Kirensky Institute of Physics, SB RAS, Krasnoyarsk 660036, Russia

<sup>g</sup> Laboratory of Nanodiagnosis and Nanolithography, Institute of Semiconductor Physics, SB RAS, Novosibirsk 630090, Russia



### ARTICLE INFO

#### Article history:

Received 21 July 2014

Received in revised form

10 September 2014

Accepted 30 September 2014

Available online 7 October 2014

#### Keywords:

- A. Inorganic compounds
- B. Chemical synthesis
- C. Photoelectron spectroscopy
- X-ray diffraction
- D. Electronic structure

### ABSTRACT

$\beta$ -RbNd(MoO<sub>4</sub>)<sub>2</sub> microplates have been prepared by the multistage solid state synthesis method. The phase composition and micromorphology of the final product have been evaluated by XRD and SEM methods. The electronic structure of  $\beta$ -RbNd(MoO<sub>4</sub>)<sub>2</sub> molybdate has been studied employing the X-ray photoelectron spectroscopy (XPS) and X-ray emission spectroscopy (XES). For the molybdate, the XPS core-level and valence-band spectra, as well as XES bands representing energy distribution of the Mo 4d- and O 2p-like states, have been measured. It has been established that the O 2p-like states contribute mainly to the upper portion of the valence band with also significant contributions throughout the whole valence-band region. The Mo 4d-like states contribute mainly to a lower valence band portion.

© 2014 Elsevier Ltd. All rights reserved.

## 1. Introduction

Molybdate crystals have become of considerable interest for detailed evaluation because of their valuable structural, luminescent and spectroscopic properties promising for practical applications in laser and photonic technologies [1–9]. The molybdates containing rare-earth elements are of special importance because of their specific spectroscopic properties [2,3,5–9]. As a rule, in the molybdates the rare-earth ions are in the low symmetry positions, and this is a key factor for creation of effective luminescent media.

A large family of binary molybdates with the general formula RbLn(MoO<sub>4</sub>)<sub>2</sub>, where Ln is a rare-earth element, was discovered many years ago [10,11]. After several initial studies, however, the observation of this crystal family was not continued. Generally, the RbLn(MoO<sub>4</sub>)<sub>2</sub> crystal family shows evident potentials for a wide range of solid solution formation and is promising for the creation of new optical materials with tunable properties [12,13]. As a representative member, RbNd(MoO<sub>4</sub>)<sub>2</sub> molybdate can be considered. The existence of two polymorphous modifications, mainly  $\alpha$  and  $\beta$  phases, was found for RbNd(MoO<sub>4</sub>)<sub>2</sub> with a phase transition occurring at  $t \sim 710$  °C [10]. Later, the phase transitions at  $t \sim 500$  °C

with small thermal effects were detected in RbLn(MoO<sub>4</sub>)<sub>2</sub> molybdates for rare-earth elements with atomic numbers ranging from 60 to 71 [14]. Then, the phase diagram of the quasi-binary Rb<sub>2</sub>MoO<sub>4</sub>–Nd<sub>2</sub>(MoO<sub>4</sub>)<sub>3</sub> system was defined for the temperature region of  $t > 500$  °C [15]. Recently, the crystal structure of the orthorhombic polymorphous modification  $\beta$ -RbNd(MoO<sub>4</sub>)<sub>2</sub> has been refined in space group *Pbcn* and the spectroscopic properties of the compound were evaluated [16]. The layered crystal structure of  $\beta$ -RbNd(MoO<sub>4</sub>)<sub>2</sub> is shown in Fig. 1, and it is related to the KY(MoO<sub>4</sub>)<sub>2</sub> type, which is well-known in binary Ln-containing molybdates with large alkali cations [16–18]. The crystal structure of polymorphous modification  $\alpha$ -RbNd(MoO<sub>4</sub>)<sub>2</sub> and the origin of the phase transition occurring at  $T \sim 500$  °C are still unclear. Other physical and chemical properties of  $\beta$ -RbNd(MoO<sub>4</sub>)<sub>2</sub> remain unknown. In comparison with  $\beta$ -RbNd(MoO<sub>4</sub>)<sub>2</sub>, other molybdates belonging to the RbLn(MoO<sub>4</sub>)<sub>2</sub> family are even less studied. Thus, the present study is aimed at the exploration of the electronic structure of  $\beta$ -RbNd(MoO<sub>4</sub>)<sub>2</sub> by X-ray photoelectron spectroscopy (XPS). Earlier, in a number of first-principles band-structure calculations of molybdates with the common formula MMoO<sub>4</sub> (M=Mg, Ni, Zn, Ba, Pb, Sr) [19–24], it has been established that their electronic structure is characterized by significant contributions of the valence O p and Mo d states throughout the whole valence band region. In the present paper, we also employ X-ray

\* Corresponding author. Fax: +7 383 3332771.

E-mail address: [atuchin@isp.nsc.ru](mailto:atuchin@isp.nsc.ru) (V.V. Atuchin).

emission spectroscopy (XES) to measure for the  $\beta$ -RbNd(MoO<sub>4</sub>)<sub>2</sub> sample the XE O K $\alpha$  and Mo L $\beta_{2,15}$  bands representing mainly energy distributions of the O 2p- and Mo 4d-like states, respectively, and to compare them, on a common energy scale, to the XPS valence-band spectrum of the molybdate under consideration.

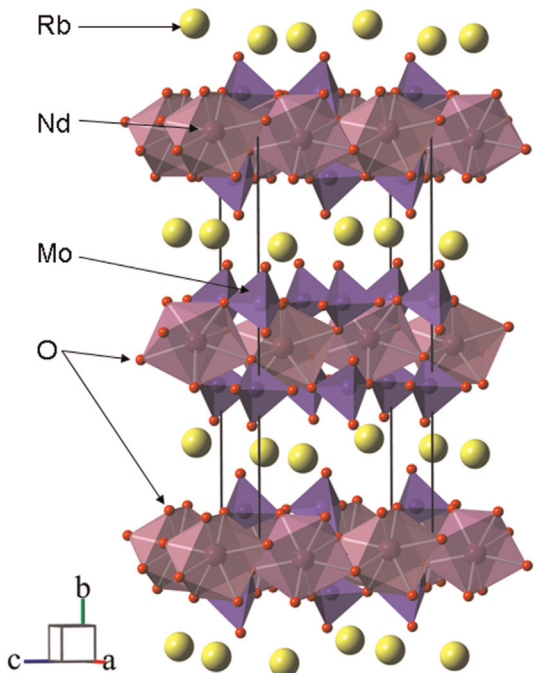


**Fig. 1.** The crystal structure of  $\beta$ -RbNd(MoO<sub>4</sub>)<sub>2</sub>, space group *Pbcn*. Lone atoms of neodymium, molybdenum and oxygen are omitted. Unit cell is outlined.

## 2. Experimental

Polycrystalline molybdate  $\beta$ -RbNd(MoO<sub>4</sub>)<sub>2</sub> has been specially derived for the present experimental studies by solid state synthesis using a stoichiometric ratio mixture of analytically pure MoO<sub>3</sub> (99.9%), Rb<sub>2</sub>CO<sub>3</sub> (99.99%), and Nd<sub>2</sub>O<sub>3</sub> (> 99.9%) as starting materials. It is well known that MoO<sub>3</sub> is relatively volatile at high temperatures and, consequently, a partial loss of this component during long time synthesis may induce deviation from the stoichiometry of synthesized compounds [25,26]. To minimize this effect, the multistage method with a step-by-step temperature increase is optimal for complex molybdates synthesis [27–29]. Therefore, initially, rubidium and neodymium molybdates were prepared by the routine ceramic technique. Heat treatment of stoichiometric mixtures was started at  $T=723$  K and followed by a step-wise temperature increasing up to  $T=873$  K (Rb<sub>2</sub>MoO<sub>4</sub>) and 1073 K (Nd<sub>2</sub>(MoO<sub>4</sub>)<sub>3</sub>). The phase purity of intermediate products Rb<sub>2</sub>MoO<sub>4</sub> and Nd<sub>2</sub>(MoO<sub>4</sub>)<sub>3</sub> was evaluated by powder XRD on a Bruker D8 ADVANCE powder diffractometer (CuK $\alpha$  radiation, secondary monochromator,  $2\theta=10^\circ$ – $70^\circ$ , scan step  $0.02^\circ$ , exposition 2 s). The XRD patterns were compared to the available structural characteristics of the molybdates [30,31]. The powder mixture of the compounds in stoichiometric ratio was being preheated at  $T=723$  K for about 50 h and then annealed at  $T=873$  K for 150 h to yield the RbNd(MoO<sub>4</sub>)<sub>2</sub> composition. The powder diffraction data of  $\beta$ -RbNd(MoO<sub>4</sub>)<sub>2</sub> for Rietveld analysis were collected at room temperature with a Bruker D8 ADVANCE powder diffractometer (Cu-K $\alpha$  radiation) and linear VANTEC detector. The step size of  $2\theta$  was  $0.016^\circ$ , and the counting time was 2 s per step. The data were collected over the angle range of  $2\theta=5^\circ$ – $100^\circ$ . Micromorphology was observed by SEM using an LEO 1430 device.

The XPS valence-band and core-level spectra of RbNd(MoO<sub>4</sub>)<sub>2</sub> were measured using the UHV-Analysis-System assembled by SPECS Surface Nano Analysis Company (Berlin, Germany). The

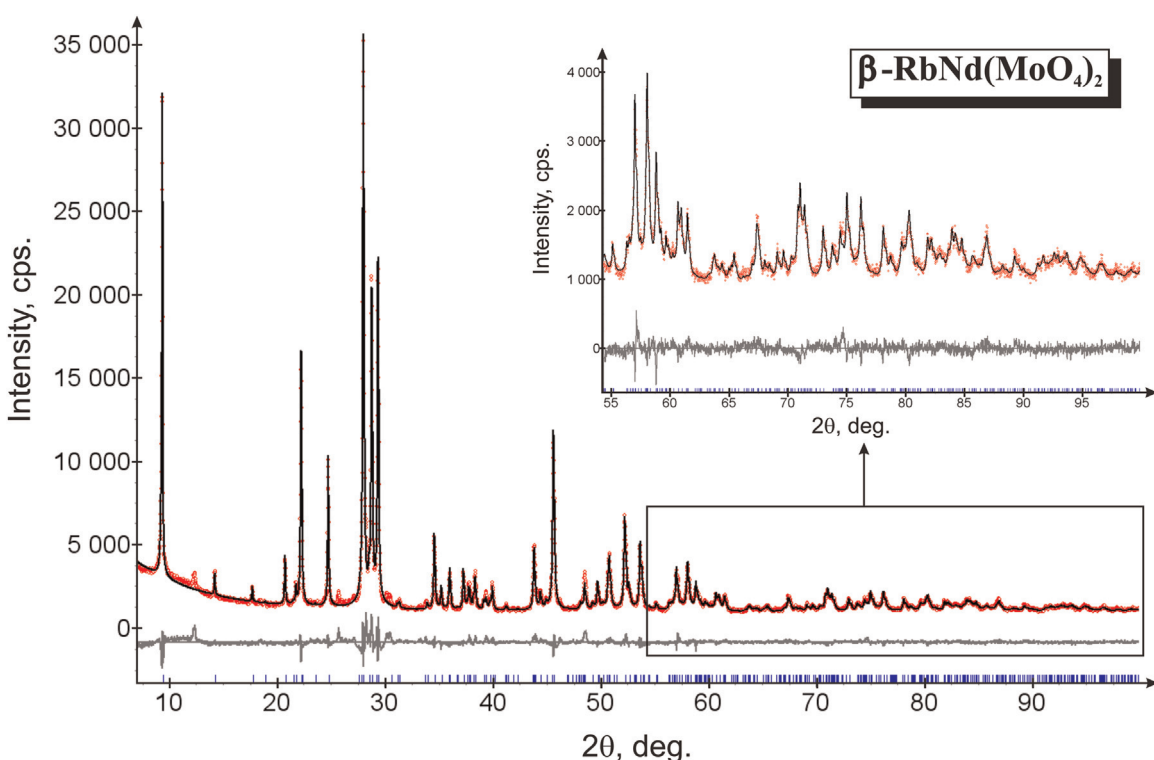


**Fig. 2.** X-ray diffraction pattern of the  $\beta$ -RbNd(MoO<sub>4</sub>)<sub>2</sub> molybdate.

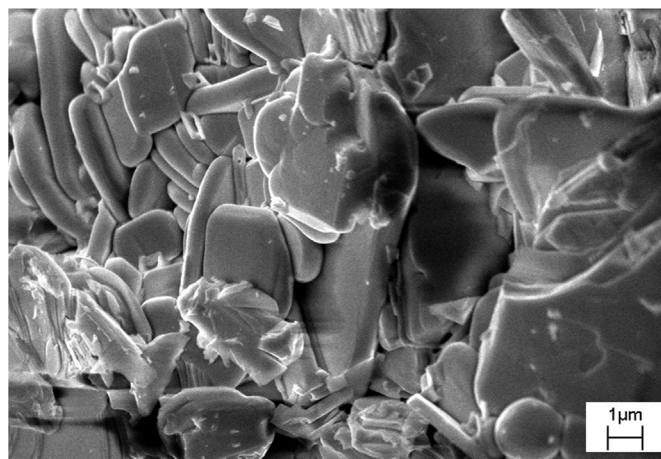


Fig. 3. SEM pattern of the  $\beta$ -RbNd( $\text{MoO}_4$ )<sub>2</sub> microparticles.

system is equipped with a PHOIBOS 150 hemispherical analyzer. A base pressure of a sublimation ion-pumped chamber of the system was less than  $4 \times 10^{-10}$  mbar during the present experiments. The Mg K $\alpha$  irradiation ( $E=1253.6$  eV) was used as a source of XPS spectra excitation. The XPS spectra were measured at the constant pass energy of 25 eV. The energy scale of the spectrometer was calibrated by setting the measured Au 4f<sub>7/2</sub> and Cu 2p<sub>3/2</sub> binding energies to  $84.00 \pm 0.05$  eV and  $932.66 \pm 0.05$  eV, respectively, in reference to Fermi energy  $E_F$ . The energy drift due to charging effects was calibrated, taking the XPS C 1s (284.6 eV) core-level spectrum of hydrocarbons as it was suggested for dielectric tungstate materials [32–35].

The fluorescent X-ray emission Mo L $\beta_{2,15}$  band ( $\text{L}_{\text{III}} \rightarrow \text{N}_{\text{IV,V}}$  transition) representing the energy distribution of mainly the Mo 4d-like states, was measured in the  $\beta$ -RbNd( $\text{MoO}_4$ )<sub>2</sub> molybdate using a Johann-type SARF-1 spectrometer employing the technique described in detail in [36]. Briefly, the dispersing element of

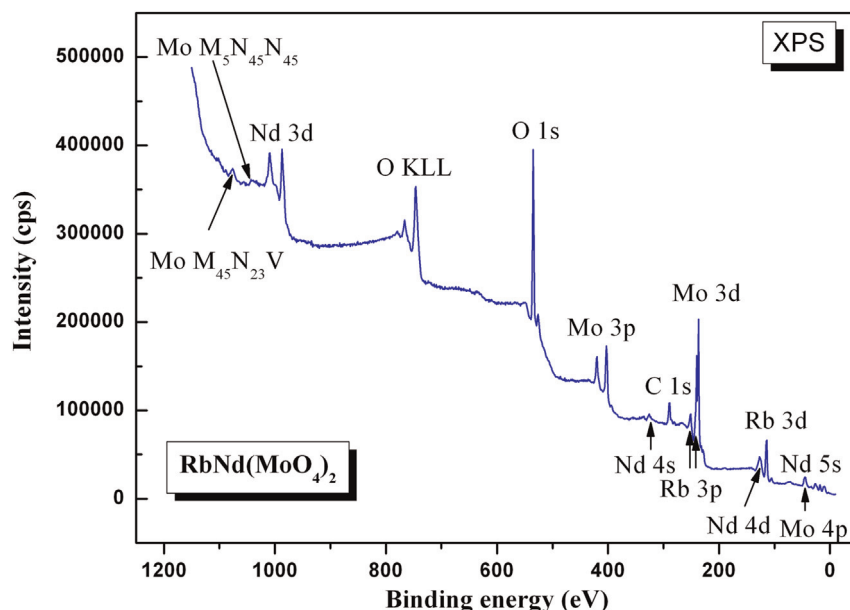


Fig. 4. Survey XPS spectrum of the  $\beta$ -RbNd( $\text{MoO}_4$ )<sub>2</sub> molybdate.

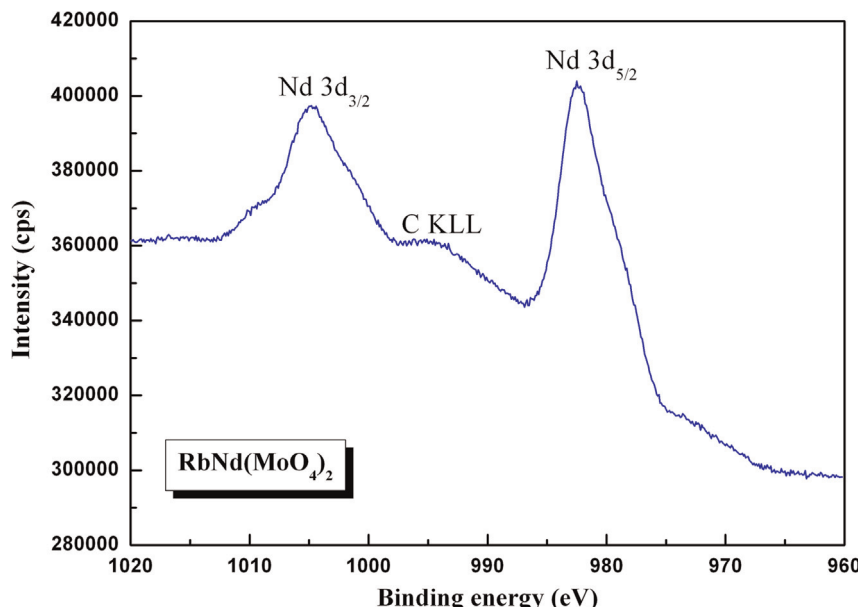


Fig. 5. Detailed XPS Nd 3d core-level spectrum and C KLL Auger line of the  $\beta$ -RbNd( $\text{MoO}_4$ )<sub>2</sub> molybdate.

the spectrometer was a quartz crystal with the  $(10\bar{1}1)$  reflecting plane and the curvature radius of  $R \approx 500$  mm. The energy resolution,  $\Delta E_{\min}$ , of the SARF-1 spectrometer in the range corresponding to the energy of the Mo  $L\beta_{2,15}$  band was found to be better than 0.4 eV. The detector was a gas flow argon-methane counter. As a source of primary excitation, an X-ray tube operating at accelerating voltage,  $U_a = 6$  kV, and anode current,  $I_a = 600$  mA, was used. The Mo  $L\beta_{2,15}$  band was recorded in a spectrometer chamber having a base pressure less than  $1 \times 10^{-6}$  Pa. The ultra-soft XE O  $K\alpha$  band ( $K \rightarrow L_{II,III}$  transition), representing the energy distribution of the O 2p-states, was measured with  $\Delta E_{\min} \approx 0.3$  eV using an RSM-500 spectrometer equipped with a diffraction grating possessing 600 lines/mm and the curvature radius of  $R = 6026$  mm. A secondary electron multiplier VEU-6 with a CsI photocathode was used as a detector. The operating conditions of a spectrometer electron gun, in the present experiments, were the following:  $U_a = 5.0$  kV,  $I_a = 2.5$  mA. The specimen was mounted on

a water-cooling anode. No changes of the XE O  $K\alpha$  band shape were observed during acquisition of the spectra.

### 3. Results and discussion

The final product of high temperature synthesis was found to be of light-purple color that is common for  $Nd^{3+}$ -containing oxides. The synthesized oxide is a single-phase material as it is evidenced from the XRD pattern shown in Fig. 2. Almost all peaks, besides three low intensity impurity peaks at  $2\theta = 12.3^\circ$ ,  $25.7^\circ$  and  $30.2^\circ$ , were indexed by orthorhombic cell ( $Pbcn$ ) with the parameters close to  $TlPr(MoO_4)_2$  [37]. Therefore, the crystal structure of  $TlPr(MoO_4)_2$  was taken as starting model for the Rietveld refinement performed by TOPAS 4.2. The refinement was stable and confirmed a good quality of the  $\beta$ -RbNd( $MoO_4$ )<sub>2</sub> sample. A small peak overlapping and the high

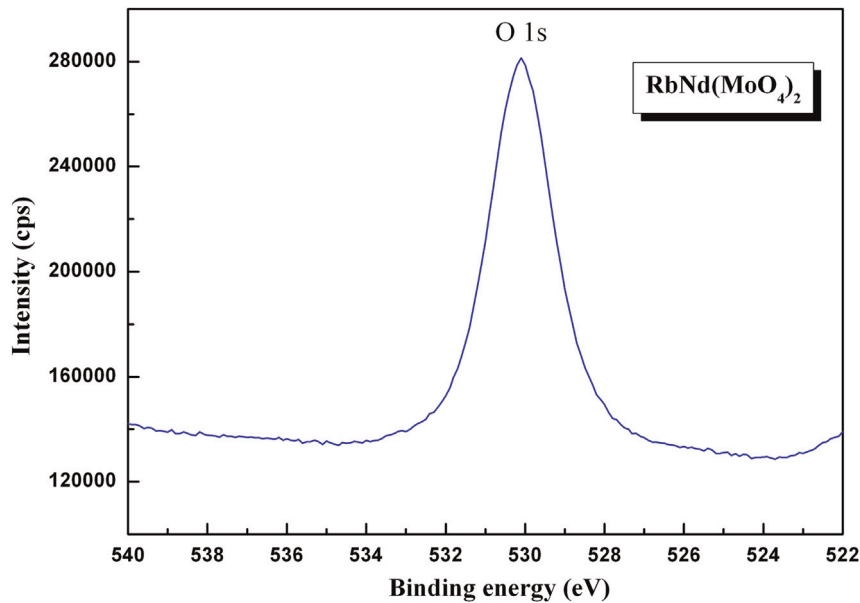


**Fig. 6.** Detailed XPS O 1s core-level spectrum of the  $\beta$ -RbNd( $MoO_4$ )<sub>2</sub> molybdate.

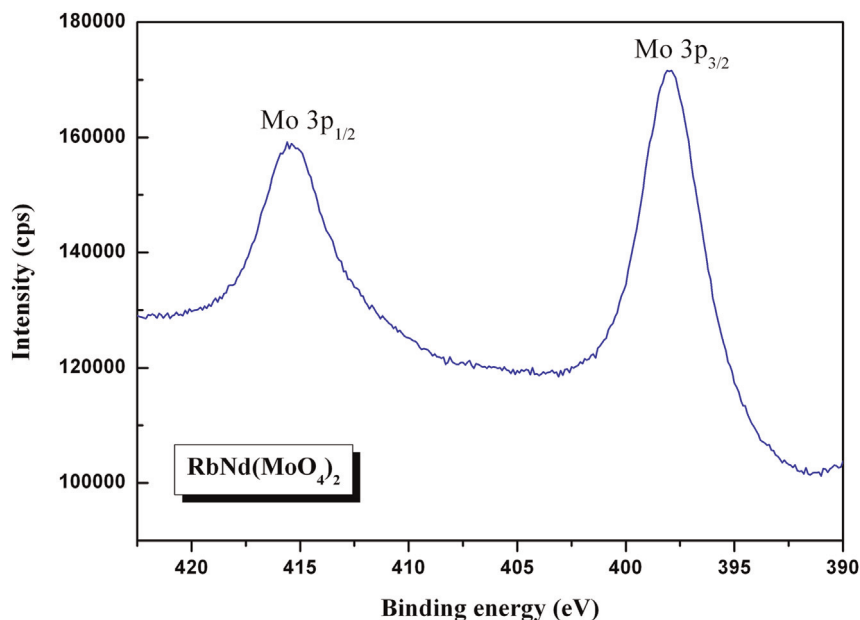


**Fig. 7.** Detailed XPS Mo 3p core-level spectrum of the  $\beta$ -RbNd( $MoO_4$ )<sub>2</sub> molybdate.

maximum value of  $2\theta=100^\circ$  allow one to define the cell parameters with a high precision:  $a=5.17673(12)$  Å,  $b=18.7310(5)$  Å,  $c=8.24593(19)$  Å, and  $V=799.57(3)$  Å<sup>3</sup>. The absence of anisotropic broadening of diffraction peaks indicates negligible size/strain effects in the micro-crystals. The morphology of the final product is shown in Fig. 3. The microparticles are formed by slightly agglomerated plate-like crystals with typical dimensions  $12 \times 6 \times 1$  μm<sup>3</sup> and smoothed edges. The crystal habit appeared to be governed by a layered structure common for the MLn(MoO<sub>4</sub>)<sub>2</sub>-type molybdates [12,13,16].

The survey XPS spectrum is shown in Fig. 4. From the figure, it is apparent that all the spectral features, except for the carbon 1s level at 284.6 eV originated from adventitious hydrocarbons adsorbed on the surface, are attributed to the constituent element core-levels or Auger lines. It should be mentioned that the relative intensity of the C 1s core-level line for the β-RbNd(MoO<sub>4</sub>)<sub>2</sub> surface under study was found to be rather weak. The relative element contents were estimated using the detailed spectra of the XPS Rb

3d, Nd 3d<sub>5/2</sub>, Mo 3d<sub>5/2</sub> and O 1s core-level lines and the tabulated data on the corresponding atomic sensitivity factors (ASF) [38]. The resulting composition Rb:Nd:Mo:O=0.075:0.069:0.188:0.668 is in good agreement with the nominal composition of Rb:Nd:Mo:O=0.08:0.08:0.17:0.67.

The superposition of the Nd 3d core-level spectra and the Auger C KLL line in β-RbNd(MoO<sub>4</sub>)<sub>2</sub> is presented in Fig. 5. However, the C KLL line is of low intensity and is not superimposed with the main Nd 3d<sub>3/2</sub> and Nd 3d<sub>5/2</sub> features. Each component of the Nd 3d<sub>5/2</sub> and Nd 3d<sub>3/2</sub> spectra, including the low intensity hump on the higher BE side of the Nd 3d<sub>3/2</sub> component, shows a multiple structure specific for Nd-bearing oxides [39–43]. This effect appears to be due to bonding and antibonding states between the 3d<sup>9</sup>4f<sup>0</sup> and 3d<sup>9</sup>4f<sup>1</sup>L configurations where L indicates the O 2p hole [39,41]. It is interesting that a comparatively simple Nd 3d doublet structure has been measured for Nd(OH)<sub>3</sub>, supposedly due to a worse apparatus resolution [44]. The shoulder that appeared on

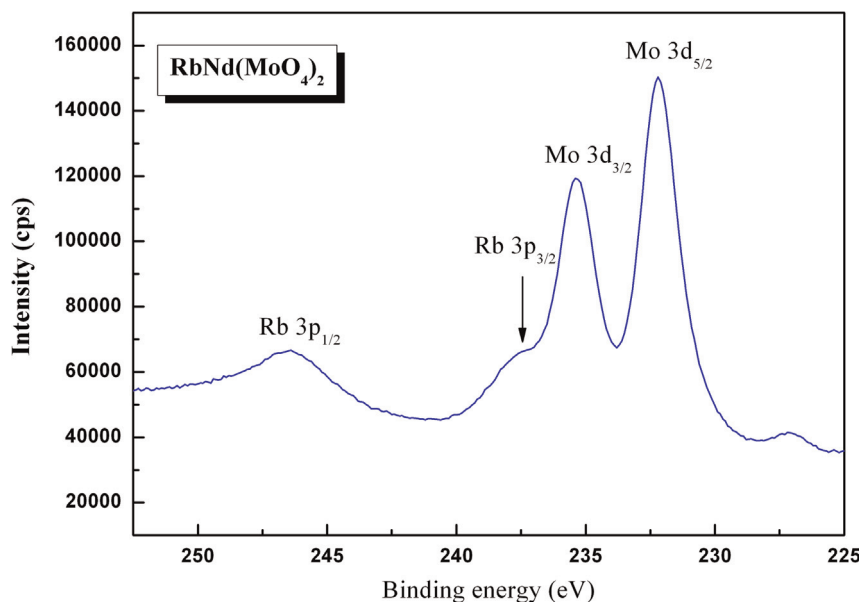


**Fig. 8.** Detailed XPS Rb 3p and Mo 3d core-level spectra of the β-RbNd(MoO<sub>4</sub>)<sub>2</sub> molybdate.

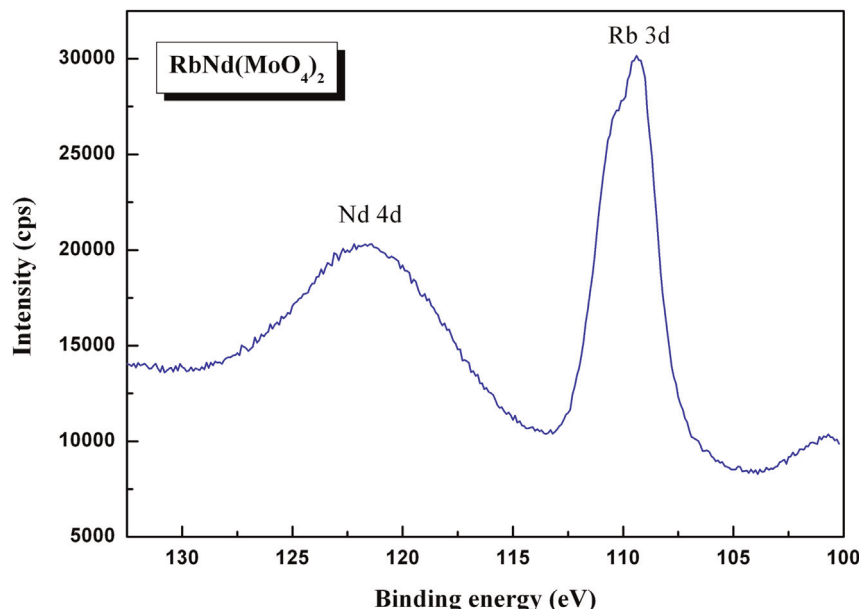


**Fig. 9.** Detailed XPS Nd 4d and Rb 3d core-level spectra of the β-RbNd(MoO<sub>4</sub>)<sub>2</sub> molybdate.

the lower BE side of the Nd 3d<sub>5/2</sub> component is attributed to O KLL Auger emission, and this signature is typically observed in the Nd-bearing oxides [38,40,41,43]. The XPS O 1 s core-level spectrum recorded for  $\beta$ -RbNd(MoO<sub>4</sub>)<sub>2</sub> is shown in Fig. 6. The shape is symmetrical and narrow, and that verifies the absence of OH-groups adsorbed on the surface. This indicates that  $\beta$ -RbNd(MoO<sub>4</sub>)<sub>2</sub> is a relatively stable compound in reference to hydration in the air. The XPS Mo 3p, Rb 3p and Mo 3d core-level spin-orbit doublets are shown in Figs. 7 and 8. The Rb 3p and Mo 3d doublets are partly superimposed in  $\beta$ -RbNd(MoO<sub>4</sub>)<sub>2</sub>. The Nd 4d and Rb 3d core-level spectra of  $\beta$ -RbNd(MoO<sub>4</sub>)<sub>2</sub> are shown in Fig. 9. The Nd 4d line is very wide and the binding energy (BE) of its maximum is typical of the Nd<sup>3+</sup> ion in oxides [41,43,44]. The Rb 3d spin-orbit doublet is not resolved, but the BE of the maximum is in the range

of BE(Rb 3d) earlier observed for the Rb<sup>+</sup> ion in different oxide compounds [45–47]. A lot of element core levels with several superpositions are found at low BE values, as it is shown in Fig. 10, where the upper XPS Nd 5s, Mo 4p, Rb 4s, Nd 5p, and O 2s core-level spectra of  $\beta$ -RbNd(MoO<sub>4</sub>)<sub>2</sub> are presented. The XPS valence-band spectrum (including upper Rb 4p core-level) is shown in Fig. 11. It is obvious from Fig. 11 that two fine-structure peculiarities, namely A and B, are well resolved in the XPS valence-band spectrum of  $\beta$ -RbNd(MoO<sub>4</sub>)<sub>2</sub>, where the mixed valence states are located (at BE < 10 eV). The total set of the BE values of the constituent element core levels and Auger lines observed from  $\beta$ -RbNd(MoO<sub>4</sub>)<sub>2</sub> is listed in Table 1.

With respect to the occupation of the electronic states associated with molybdenum and oxygen atoms in the valence-band

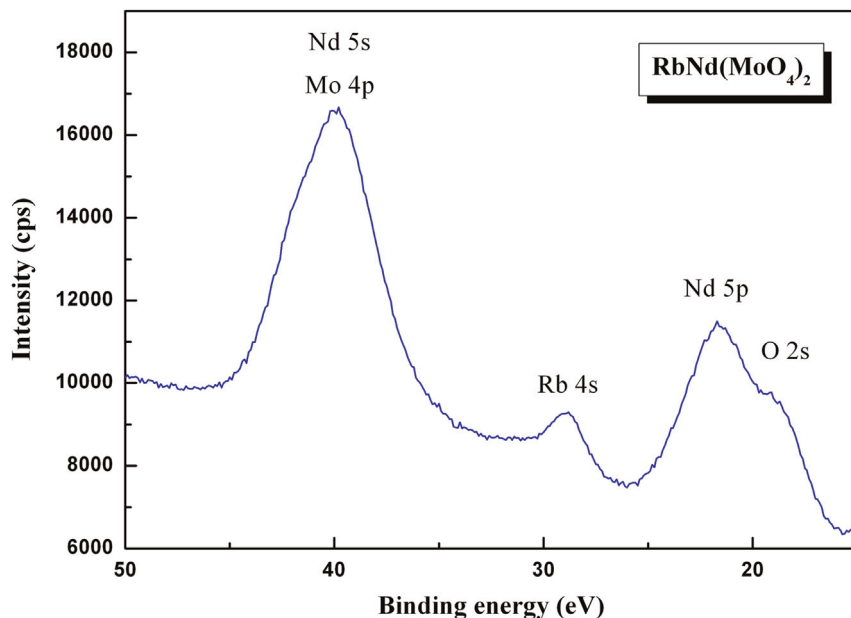


**Fig. 10.** Detailed upper XPS Nd 5s, Mo 4p, Rb 4s, Nd 5p, O2s core-level spectra of the  $\beta$ -RbNd(MoO<sub>4</sub>)<sub>2</sub> molybdate

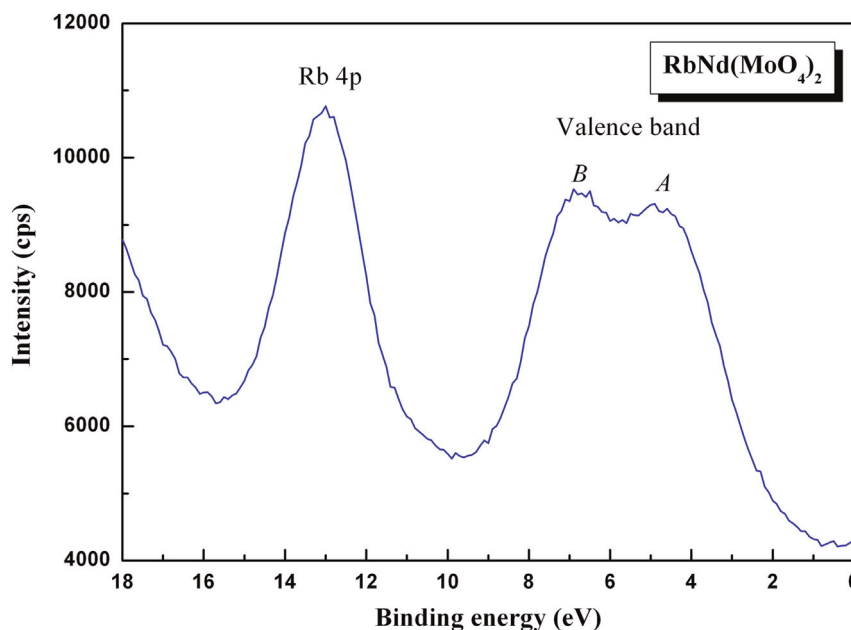


**Fig. 11.** Detailed XPS valence-band spectrum of the  $\beta$ -RbNd(MoO<sub>4</sub>)<sub>2</sub> molybdate.

**Table 1**

Binding energies ( $\pm 0.05$  eV) of the constituent element core levels and Auger lines in  $\beta\text{-RbNd}(\text{MoO}_4)_2$ .

Core level, Auger line	Binding energy (eV)
VB (fine-structure features A and B)	4.9 and 6.8 <sup>a</sup>
Rb 4p	13.07
O 2s	19.3 <sup>a</sup>
Nd 5p	21.61
Rb 4s	28.93
Nd 5s + Mo 4p	40.02
Rb 3d	109.45
Nd 4d	121.6 <sup>a</sup>
Mo 3d <sub>5/2</sub>	232.19
Mo 3d <sub>3/2</sub>	235.37
Rb 3p <sub>3/2</sub>	237.5 <sup>a</sup>
Rb 3p <sub>1/2</sub>	246.42
C 1s	Fixed at 284.6
Mo 3p <sub>3/2</sub>	398.06
Mo 3p <sub>1/2</sub>	415.45
O 1s	530.11
O KLL	741.9 <sup>a</sup>
Nd 3d <sub>5/2</sub>	984.44
C KLL	994.3 <sup>a</sup>
Nd 3d <sub>3/2</sub>	1004.87

<sup>a</sup> Uncertainty of the measurements is  $\pm 0.1$  eV.

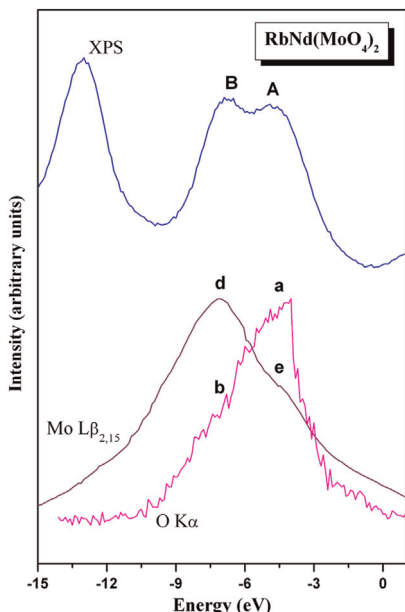


**Fig. 12.** Comparison on a common energy scale of the X-ray emission Mo  $\text{L}\beta_{2,15}$  and O  $\text{K}\alpha$  bands, as well as the XPS valence-band spectrum of the  $\beta\text{-RbNd}(\text{MoO}_4)_2$  molybdate.

region of  $\beta\text{-RbNd}(\text{MoO}_4)_2$ , the XPS valence-band spectrum and XES Mo  $\text{L}\beta_{2,15}$  and O  $\text{K}\alpha$  bands of the  $\beta\text{-RbNd}(\text{MoO}_4)_2$  molybdate, provided at a common energy scale, are shown in Fig. 12. The method of matching the above XES and XPS spectra on a common energy scale is analogous to that applied successfully in a recent study of the electronic structure of molybdenum oxides [48]. Regrettably, the available facilities do not enable the measurements of the X-ray emission bands giving information about energy distribution of the valence states associated with Rb and Nd atoms. The results presented in Fig. 12 reveal that, in the  $\beta\text{-RbNd}(\text{MoO}_4)_2$  double molybdate, the main contributions of the Mo 4d- and O 2p-like states appear at the bottom and near the top of the valence band, respectively, with contributions of the mentioned states throughout other valence band portions. The results are consistent with theoretical band-structure calculations

of molybdates with the common formula  $\text{MMoO}_4$  ( $\text{M} = \text{Mg, Ni, Zn, Ba, Pb, Sr}$ ) [19–24] and resemble experimental findings for molybdenum trioxide  $\text{MoO}_3$ [48], as well as those for other higher transition metal oxides, particularly  $\text{TiO}_2$ [49],  $\text{V}_2\text{O}_5$ [50] and  $\text{WO}_3$  [51]. As can be seen from Fig. 12, the comparison on a common energy scale of the XES and XPS spectra of  $\beta\text{-RbNd}(\text{MoO}_4)_2$  shows that the maximum d of the Mo  $\text{L}\beta_{2,15}$  band coincides with the low-energy feature b of the O  $\text{K}\alpha$  band and the maximum B of the XPS valence-band spectrum. The main maximum a of the O  $\text{K}\alpha$  band, coinciding with the feature A of the XPS valence-band spectrum, superimposes the broad low-energy shoulder of the Mo  $\text{L}\beta_{2,15}$  band. Earlier, it was established for the orthorhombic molybdenum trioxide that the feature b of the O  $\text{K}\alpha$  band is formed by contributions of the O  $2p_\sigma$ -like states, while the O  $2p_\pi$ -like states contribute mainly to the maximum a of the O  $\text{K}\alpha$  band [48]. It is worth mentioning that the electronic structure of the  $\beta\text{-RbNd}(\text{MoO}_4)_2$  molybdate resembles somewhat that of the double tungstate  $\alpha\text{-KY(WO}_4)_2$  [52]. In the latter work, it has been established that the O 2p- and W 5d-like states contribute mainly to the upper and lower  $\text{KY(WO}_4)_2$  valence band portions with also significant contributions throughout the whole valence-band region. The similar feature is characteristic for the electronic structure of the  $\beta\text{-RbNd}(\text{MoO}_4)_2$  molybdate as it has been already mentioned above.

#### 4. Conclusions

A high-quality  $\beta\text{-RbNd}(\text{MoO}_4)_2$  molybdate has been synthesized and its electronic structure has been studied for the first time employing X-ray photoelectron spectroscopy (XPS) and X-ray emission spectroscopy (XES). Constituent element core levels and Auger lines in this complex molybdate have been measured with XPS. The measurement results of the X-ray emission bands representing energy distribution of the Mo 4d- and O 2p-like states, that were matched on a common energy scale with the X-ray photoelectron spectrum of the molybdate studied, indicate that the O2p- and Mo 4d-like states contribute mainly to the upper and lower valence band portions, respectively. General similarity has been found in the valence band structures of  $\beta\text{-RbNd}(\text{MoO}_4)_2$  and  $\alpha\text{-KY(WO}_4)_2$  by comparative analysis. Thus, it seems to be a general feature of molybdates and tungstates that the valence band top is dominated by O2p-like states, and Mo 4d- or W 5d-like states contribute mainly to the lower energy parts of the valence band in molybdates and tungstates, respectively.

#### Acknowledgements

This study was partially supported by the Ministry of Education and Science of the Russian Federation and RFBR Grant 12-02-90806-mol\_rf\_nr.

#### References

- [1] T.T. Basiev, A.A. Sobol, Yu.K. Voronko, P.G. Zverev, Spontaneous Raman spectroscopy of tungstate and molybdate crystals for Raman lasers, Opt. Mater. 15 (2000) 205–216.
- [2] A. Brenier, D. Jaque, A. Majchrowski, Bi-functional laser and non-linear optical crystals, Opt. Mater. 28 (4) (2006) 310–323.
- [3] Zhiguo Xia, Daimei Chen, Synthesis and luminescence properties of  $\text{BaMoO}_4$ :  $\text{Sm}^{3+}$  phosphors, J. Am. Ceram. Soc. 93 (5) (2010) 1397–1401.
- [4] Victor Atuchin, Lei Zhu, Soo Hyun Lee, Dae Hyun Kim, Chang Sung Lim, Microstructure and optical properties of  $\text{BaMO}_4$  ( $\text{M} = \text{Mo, W}$ ) particles synthesized by microwave-assisted metathetic method, Asian J. Chem. 26 (5) (2014) 1293–1296.

